



## Letter

# Variations in an oleic acid and metal nitrate emulsion under calcination on the structural and morphology of LaAlO<sub>3</sub> nanopowders

J. Chandradass, M. Balasubramanian, Dong-Sik Bae, Jongryoul Kim, Ki Hyeon Kim\*

Department of Physics, Yeungnam University, Gyeongsan, Gyeongsangbuk-do-712-749, South Korea  
 Department of Metallurgical and Materials Engineering, Indian Institute of Technology-Madras, Chennai 600036, India  
 School of Nano and Advanced Material Engineering, Changwon National University, Gyeongnam 641-773, South Korea  
 Department of Metallurgical and Materials Engineering, Hanyang university, Ansan 425-791, South Korea  
 Department of Physics, Yeungnam University, Gyeongsan, Gyeongsangbuk-do-712-749, South Korea

## ARTICLE INFO

## Article history:

Received 6 August 2009

Received in revised form 12 March 2010

Accepted 13 March 2010

Available online 18 March 2010

## Keywords:

Ceramics

Chemical synthesis

Microstructure

X-ray diffraction

Transmission electron microscopy

## ABSTRACT

In this paper, we describe variations in an oleic acid and metal nitrate emulsion during the process of forming superfine LaAlO<sub>3</sub> crystallites from the mixture of oleic acid and metal nitrate precursors. The influence of oleic acid to metal nitrate ratio (ol/mn) on the phase and morphology were characterized by Differential thermal analysis (DTA-TGA), X-ray diffraction (XRD) and transmission electron microscopy (TEM). X-ray diffraction analysis of the powders with ol/mn ≤ 1 indicated the formation of pure rhombohedral LaAlO<sub>3</sub> at 800 °C. The optimal ratio of the oleic acid to metal nitrate for preparing fine LaAlO<sub>3</sub> nanopowders of 29 nm was 0.5. The TEM micrographs indicated morphological change (sphere, cube, triangle, etc.) as the oleic acid to metal nitrate ratio increases from 0.5 to 2.

© 2010 Elsevier B.V. All rights reserved.

## 1. Introduction

LaAlO<sub>3</sub> with a perovskite-type structure has good dielectric characteristics: high relative permittivity ( $\epsilon_r = 23$ ), high quality factor ( $Q \times f \approx 68,000$ ;  $Q = 1/\tan \delta$ ;  $f$ : measuring frequency and  $\tan \delta$ : dissipation factor), and a very small temperature coefficient of resonant frequency ( $\tau_f = -44 \times 10^{-6} \text{ } ^\circ\text{C}^{-1}$ ) [1]. This material can be used for dielectric resonators [1], substrate and insulating buffer for high-temperature superconducting microwave device [2], catalyst or catalyst support [3], electrolyte or electrode for solid oxide fuel cells [4], doped with some rare-earth ions are very promising nanophosphor materials [5] etc. Hreniak et al. [6] have discussed the synthesis and luminescence properties of LaAlO<sub>3</sub>:Eu<sup>3+</sup>. They have pointed out the increasing luminescence lifetime with decreasing nanocrystal size. Kuo et al. [7] have prepared LaAlO<sub>3</sub> by chemical co precipitation at 700 °C for 6 h. Ran and Gao [8] have reported that by pyrolysis of complex compounds of lanthanum and aluminium with triethanolamine, pure perovskite LaAlO<sub>3</sub> has been obtained when the precursor is heat-treated in a furnace at 750 °C for 4 h. Negahdari et al. [9] prepared LaAlO<sub>3</sub> nanopowders by sucrose method at 800 °C for 2 h. Tian et al. [10] prepared LaAlO<sub>3</sub> by reverse micro-emulsion method at 800 °C for

2 h. Chandradass and Kim [11] have also prepared LaAlO<sub>3</sub> by reverse micelle method and studied the effect of water-to-surfactant ratio on the particle size. In our previous study, we have prepared LaAlO<sub>3</sub> nanopowders by emulsion combustion method with average particle size of about 60 nm [12]. Although emulsion combustion method has been used to synthesis this material, some improvement or optimization of parameter is still required to control the particle size for commercial application.

Emulsion combustion (EC), a novel processing method for making a fine powder comprises preparing an emulsion formed between water-immiscible organic fluid and aqueous solutions of precursor. In this process, metal ions present in the aqueous droplets are rapidly oxidized by the combustion of the surrounding flammable liquid. The small reaction field and short reaction period lead to the formation of nano-size ceramic particles [13]. This technology also known as *calcination control of chemical additives* (CCCA), has been used by researchers for the preparation of BaTiO<sub>3</sub> [14], Al<sub>2</sub>O<sub>3</sub> [15–17], ZrO<sub>2</sub> [18],  $\alpha$ -Al<sub>2</sub>O<sub>3</sub>-t-ZrO<sub>2</sub> [19], LiCoO<sub>2</sub> [20], Yttria stabilized zirconia [21], ZrO<sub>2</sub>-CeO<sub>2</sub> [22], ZnO [23], Fe<sub>2</sub>O<sub>3</sub> [23], CeO<sub>2</sub> [23], MgO [23] and ZnO-SiO<sub>2</sub> [24] fine powders. It is noteworthy that this procedure provides a unique and desirable situation for limiting the growth of the crystal sizes from unnecessary enlargement, seemingly caused by the incomplete combustion of the organics and the presence of char particles [17]. This method could obtain very fine nano-sized LaAlO<sub>3</sub> with a favorable range of particle size near 30 nm. Previous workers have reported oleic

\* Corresponding author. Tel.: +82 53 810 2334; fax: +82 53 810 4616.  
 E-mail address: [kee1@ynu.ac.kr](mailto:kee1@ynu.ac.kr) (K.H. Kim).

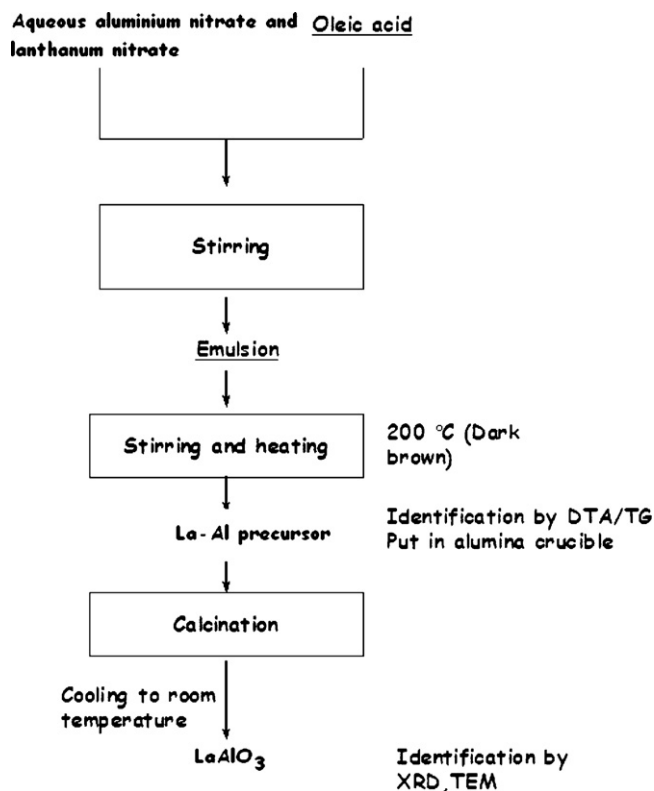


Fig. 1. Flow sheet for the preparation of nano  $\text{LaAlO}_3$ .

acid as the surfactant to modify the surface properties of  $\text{Al}_2\text{O}_3$ , aluminium, and aluminium alloys [25,26]. However, some variations in the phase transformation and morphology of La–Al precursor with organic compounds such as oleic acid are expected under calcination. The current work is in a niche of area of research in the sense that, to the best of our knowledge, there are no reports on the variations of oleic acid to metal nitrate ratios on the structural and morphology of  $\text{LaAlO}_3$  by solution combustion route. The optimal ratio of the oleic acid to metal nitrate for preparing fine  $\text{LaAlO}_3$  nanopowders of 29 nm and also the change of morphology from spherical shape to cube, triangle, etc. particles was fixed by carrying out a series of experiment.

## 2. Experimental procedures

The main procedure for the present study consisted of three steps: preparation of the aqueous precursor solution, (ii) formation of the emulsion, and (iii) the calcination process. Fig. 1 shows a flow chart of the experimental procedure for this study, which included the crucial steps of forming the emulsion, adding the surfactant oleic acid to the La–Al precursor, and mixing homogeneously. The experiments were carried out in the same way, as reported elsewhere for the preparation  $\text{Al}_2\text{O}_3$  nanopowders [15,16].

A detailed description of the three steps follows.

### 2.1. Preparation of La–Al precursor solution

Aluminium nitrate ( $\text{Al}(\text{NO}_3)_3 \cdot 9\text{H}_2\text{O}$ , Aldrich, USA) and Lanthanum (III) nitrate hexa hydrate ( $\text{La}(\text{NO}_3)_3 \cdot 6\text{H}_2\text{O}$ , Aldrich, USA) was dissolved in distilled water separately. The La-containing solution was added to the Al-containing solution in the molar ratio 1:1.

### 2.2. Formation of emulsion

Oleic acid ( $\text{C}_{17}\text{H}_{33}\text{COOH}$ , Aldrich, USA) was mixed with the La–Al precursor solution, using a magnetic stirrer. The molar ratio of oleic acid to metal nitrate was 0.5, 1, 2 and 4. The mixing speed was 1000 rpm (rotations per minute), with a duration of 30 min.

### 2.3. Calcination process

The mixed emulsion was stirred and heated in a plate heater at  $200^\circ\text{C}$  to remove water, and at the end of the mixing–heating operation, the emulsion micelles were found to have yielded dark brownish lanthanum aluminate precursor powders. The lanthanum aluminate precursor was placed into a crucible and calcinations treatment was performed at  $800^\circ\text{C}$  for 2 h.

### 2.4. Characterization

The thermal decomposition and crystallization behavior was studied using TGA-DTA (STA 1500). The phase identification of calcined powders was recorded by X-ray diffractometer (Philips X'pert MPD 3040) with a Cu target. The crystal morphology and size of the calcined powders were determined by transmission electron microscope (JEM 2100F). The chemical compositions of the crystallized powders were analyzed by a scanning electron microscopy (Hitachi Ltd., S-4200) equipped with chemical micro-analyzer by energy dispersive X-ray (EDX) analysis.

## 3. Results and discussion

### 3.1. Thermal decomposition of the precursor

The TG and DTA curves of the precursors that were obtained by heating from  $25^\circ\text{C}$  to  $1200^\circ\text{C}$  at a rate of  $10^\circ\text{C}/\text{min}$  in an air atmosphere are given in Figs. 2 and 3. An endothermic peak was noted between  $25^\circ\text{C}$  and  $100^\circ\text{C}$  on the DTA curve, representing the elimination of adsorptive water, and an exothermic peak between  $200^\circ\text{C}$  and  $700^\circ\text{C}$ , seemingly due to the decomposition of oleic acid [16]. The sharp exothermic peak at  $826^\circ\text{C}$ ,  $840^\circ\text{C}$ ,  $844^\circ\text{C}$ ,  $839^\circ\text{C}$  for oleic acid to metal nitrate with a (ol/mn) ratio of 0.5, 1, 2 and 4 is due to the formation of the  $\text{LaAlO}_3$  crystals. It was found that the exothermic peak shifts to high temperature with increase in oleic acid to metal nitrate ratio from 0.5 to 1. According to Lin and Wen [27], the emulsion system of water in oil (W/O) and the condition of adsorption to form carbon (oleic acid chars) at the oleic acid boiling point delays the  $\text{LaAlO}_3$  phase transformation. Further increase of oleic acid to metal nitrate ratio (ol/mn > 1) show negligible effect on the phase transformation temperature.

### 3.2. Phase transformation

The XRD patterns of the as-synthesized precursor powders and those calcined at  $800^\circ\text{C}$  are shown in Figs. 4 and 5. The

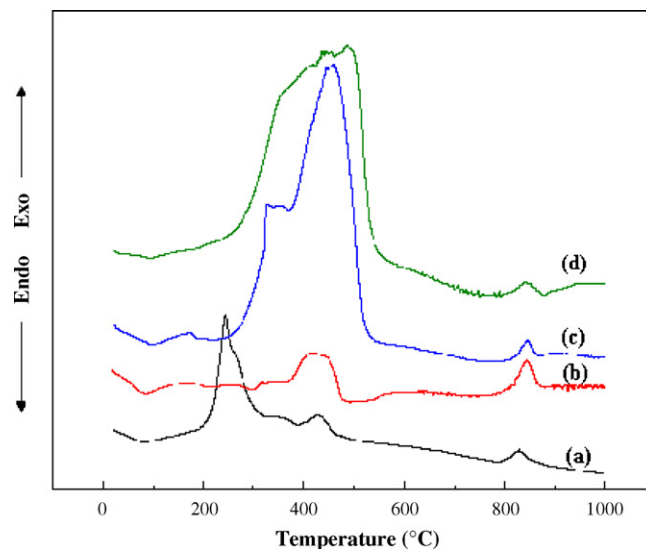
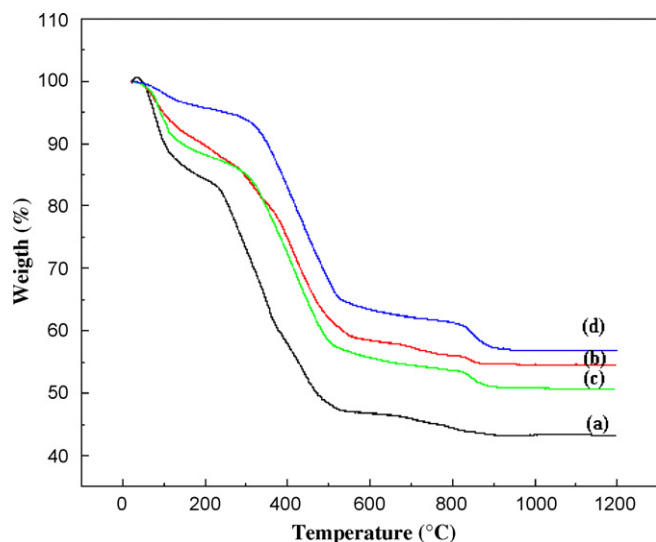
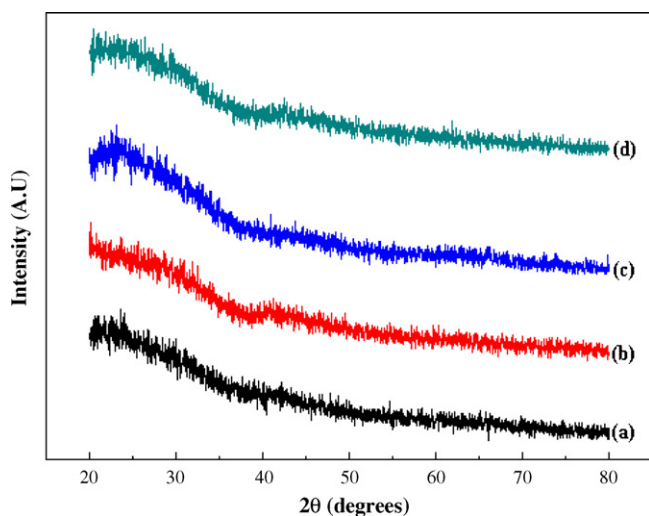


Fig. 2. Differential thermal analysis (DTA) curves of the La–Al precursor prepared by mixing aqueous metal nitrate solution and oleic acid at an (ol/mn) emulsion ratio of (a) 0.5; (b) 1; (c) 2; (d) 4.



**Fig. 3.** Thermogravimetric analysis (TGA) curves of the La–Al precursor prepared by mixing aqueous metal nitrate solution and oleic acid at an (ol/mn) emulsion ratio of (a) 0.5; (b) 1; (c) 2; (d) 4.

as-synthesized precursor powder was primarily amorphous in structure and no distinct crystallinity phase could be detected. When calcined at 800 °C for 2 h, La–Al precursor with ol/mn  $\leq 1$  seems to have transformed to pure rhombohedral  $\text{LaAlO}_3$  with a perovskite structure, as signaled by the diffraction intensity, with such crystal planes as (0 1 2), (1 1 0), (2 0 2), (0 2 4), (1 2 2), (3 0 0), (2 0 8), (3 1 2). Although  $\text{La}_2\text{O}_3$ ,  $\text{Al}_2\text{O}_3$  and  $\text{LaAl}_{11}\text{O}_{18}$  might present as intermediate phases in the course of synthesis of  $\text{LaAlO}_3$  powders, only  $\text{LaAlO}_3$  phase is detected and no intermediate phase is observed in the sample calcined at 800 °C [8]. However, the formation of minor amount of impurity ( $\text{La}_2\text{O}_3$ ) for sample with ol/mn  $> 1$  was detected. The reason is that the emulsion creates lanthanum oleate and aluminium oleate during calcinations by adsorption of oleic acid, stabilizes the oleic acid itself and helps generate carbon [27]. The carbon segregates the growth mechanism resulting in intermediate phase formation at oleic acid to metal nitrate ratio greater than 1.



**Fig. 4.** XRD patterns of the La–Al precursor prepared by mixing aqueous metal nitrate solution and oleic acid (a) ol/mn=0.5; (b) ol/mn=1; (c) ol/mn=2; (d) ol/mn=4.

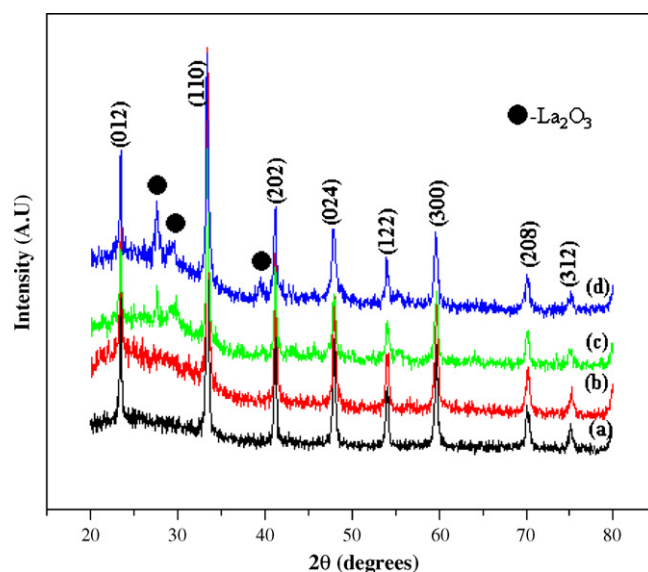
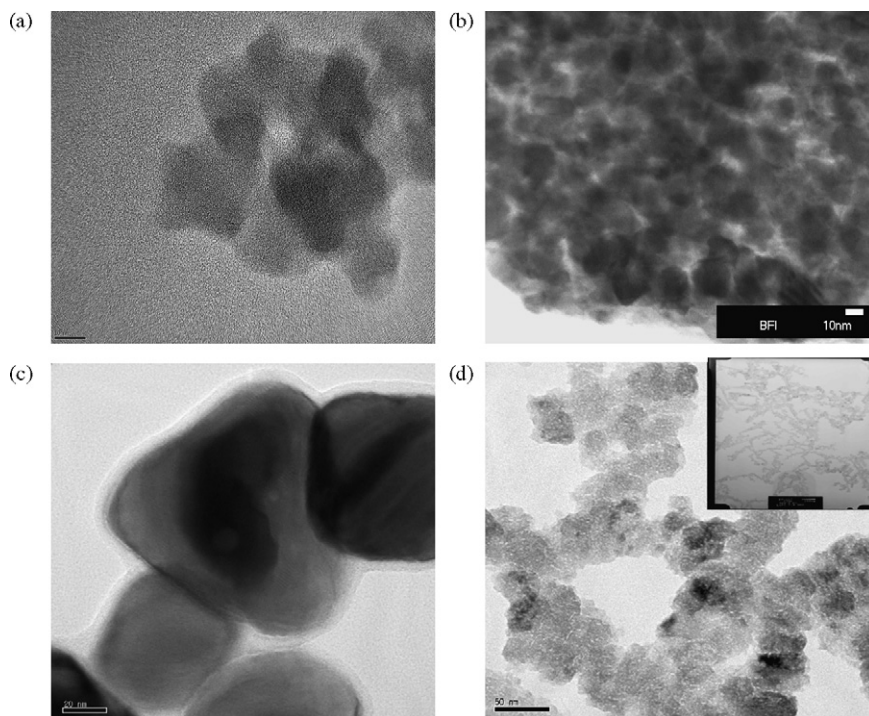


**Fig. 5.** XRD patterns of the La–Al precursor prepared by mixing aqueous metal nitrate solution and oleic acid and calcined at 800 °C (a) ol/mn=0.5; (b) ol/mn=1; (c) ol/mn=2; (d) ol/mn=4.

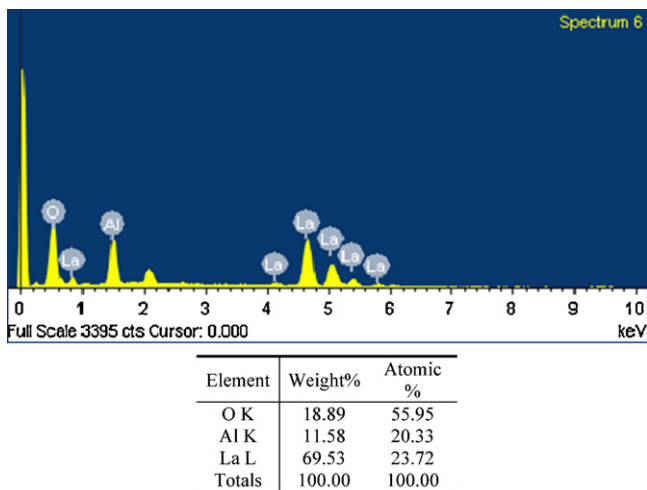
### 3.3. Morphology of $\text{LaAlO}_3$ nanopowder

Fig. 6 shows TEM micrographs of  $\text{LaAlO}_3$  nanopowder calcined at 800 °C. Initially, nucleation results in the formation of spherical nanoparticles. The change in particle morphology from spherical to cube, triangle and self assembling of nanoparticles is an excellent example of the surfactant templating of nanoparticle morphology during synthesis. The morphology change observed in the present study is due to the changes in aggregation as a function of oleic acid to metal nitrate ratio. According to Bourrel and Schester [28], when the surfactant content in the continuous phase is progressively increased to an order of magnitude higher than that corresponding to the Critical Micelle Concentration (CMC), various factors get involved, e.g. the nature of the continuous (and dispersed, when an emulsion is considered) phase, the nature of the surfactant (e.g. cationic, anionic, non-ionic) and its interaction with the continuous phase, and presence or absence of co-surfactants and/or electrolytes. However, in general it is taken for granted that at CMC, spherical or near-spherical micelles are formed. With increase in surfactant content, the molecules self-aggregate to rod-like shapes which can have end cappings. As reported elsewhere [29] that a spherical micelle in a sol-organic, i.e. W/O emulsion will have its inner space filled by the aqueous phase (sol pool) with the hydrophilic heads of the surfactant molecules pointing inside. The low aggregation number and sphericity of such micelles dictate the nanometric size and spherical shape of the ceramic particles, respectively. When the aggregation is rod-shaped, the internal space will still contain a rod-shaped sol pool, transformable to a rod-like particle after thermal treatment. Other shapes (on increasing the surfactant content) do not always offer straightforward possibilities of harboring sol pools inside them. In the present letter, a preliminary investigation has been carried out on the formation of  $\text{LaAlO}_3$  particles of different shapes by changing the ratio of oleic acid to metal nitrate. However, exact template for such shapes is yet to be assigned. This requires experimentation on the interstitial shapes with hydrophilic surfactant heads at their boundaries, so that sol pools of specific shapes can be accommodated in such interstices.

EDS was performed to further confirm the composition of calcined  $\text{LaAlO}_3$  nanopowders prepared at an ol/mn ratio of 4. Fig. 7 shows that the product is composed of La, Al and O with a mole



**Fig. 6.** TEM micrographs of the La–Al precursor prepared by mixing aqueous metal nitrate solution and oleic acid and calcined at 800 °C (a) ol/mn=0.5; (b) ol/mn=1; (c) ol/mn=2; (d) ol/mn=4.



**Fig. 7.** EDAX analysis of calcined LaAlO<sub>3</sub> nanopowders prepared at an ol/mn ratio of 4.

ratio of 1.19:1.02:2.80, which is slightly deviated to the expected 1:1 stoichiometry.

#### 4. Conclusions

The effect of oleic acid to metal nitrate emulsion ratios under calcination during the process of forming superfine LaAlO<sub>3</sub> crystallites has been studied. The optimal ratio of the oleic acid to metal nitrate for preparing fine LaAlO<sub>3</sub> nanopowders of 29 nm was 0.5. The TEM micrographs indicated morphological change (sphere, cube, triangle, etc.) as the oleic acid to metal nitrate ratio increases from 0.5 to 2.

#### References

- [1] S.Y. Cho, I.T. Kim, K.S. Hong, *J. Mater. Res.* 14 (1999) 114–119.
- [2] R.W. Simon, C.E. Platt, A.E. Lee, G.S. Lee, K.P. Daly, M.S. Wire, J.A. Luine, M. Urbanik, *Appl. Phys. Lett.* 53 (1988) 2677–2680.
- [3] R. Spinicci, P. Marini, S.D. Rossi, M. Faticanti, P. Porta, *J. Mol. Catal. A: Chem.* 176 (2001) 253–265.
- [4] T. Takahashi, H. Iwahara, *Energy Convers.* 11 (1971) 105–111.
- [5] H. Chander, *Mater. Sci. Eng. R* 49 (2005) 113–155.
- [6] D. Hreniak, W. Streck, P. Deren, A. Bednarkiewicz, A. Lukowiak, *J. Alloys Compd.* 408–412 (2006) 828–830.
- [7] C.-L. Kuo, C.-L. Wang, T.-Y. Chen, G.-J. Chen, I.-M. Hung, C.-J. Shih, K.-Z. Fung, *J. Alloys Compd.* 440 (2007) 367–374.
- [8] S. Ran, L. Gao, *Ceram. Int.* 34 (2008) 443–446.
- [9] Z. Negahdari, A. Saberi, M. Willert-Porada, *J. Alloys Compd.* 485 (2009) 367–371.
- [10] Z. Tian, W. Huang, Y. Liang, *Ceram. Int.* 35 (2009) 661–664.
- [11] J. Chandradass, K.H. Kim, *J. Cryst. Growth* 311 (2009) 3631–3635.
- [12] J. Chandradass, Ki Hyeon Kim, *J. Alloys Compd.* 481 (2009) L31–L34.
- [13] Ned E. Cipollini, N.J. Succasunnam, Emulsion-char method for making fine powder, United States Patent 4,654,075, 1987.
- [14] G.H. Maher, C.E. Hutchins, S.D. Ross, *Am. Ceram. Soc. Bull.* 72 (1993) 72–76.
- [15] Y. Sarikaya, M. Akinc, *Ceram. Int.* 14 (1988) 239–244.
- [16] C.-P. Lin, S.-B. Wen, T.-T. Lee, *J. Am. Ceram. Soc.* 85 (2002) 129–133.
- [17] Y.-C. Chen Lee, S.-B. Wen, L. Wenglin, *J. Am. Ceram. Soc.* 90 (2007) 1723–1727.
- [18] S.D. Ramamurthi, Z. Xu, D.A. Payne, *J. Am. Ceram. Soc.* 73 (1990) 2760–2763.
- [19] J. Chandradass, Dong-Sik Bae, *J. Alloys Compd.* 469 (2009) L10–L12.
- [20] S.-T. Myung, N. Kumagai, S. Komaba, H.-T. Chung, *J. Appl. Electrochem.* 30 (2000) 1081–1085.
- [21] D.S. Patil, K. Prabhakaran, C. Durgaprasad, N.M. Gokhale, A.B. Samui, S.C. Sharma, *Ceram. Int.* 35 (2009) 515–519.
- [22] K. Takatori, T. Tani, N. Watanabe, N. Kamiya, *J. Nanoparticle Res.* 1 (1999) 197–204.
- [23] T. Tani, N. Watanabe, K. Takatori, *J. Am. Ceram. Soc.* 86 (2003) 898–904.
- [24] T. Tani, N. Watanabe, K. Takatori, *J. Nanoparticle Res.* 5 (2003) 39–46.
- [25] R.A. Ross, R. Lemay, *Surf. Technol.* 26 (1985) 125–136.
- [26] B.F. Lewis, M. Mosesman, W.H. Weinberg, *Surf. Sci.* 41 (1974) 142.
- [27] C.-P. Lin, S.-B. Wen, J. Am. Ceram. Soc. 85 (2002) 1467–1472.
- [28] M. Bourrel, R.S. Schester, *Microemulsions and Related Systems*, Reinhold Publishing Corporation, New York, 1988.
- [29] D. Ganguli, *Bull. Mater. Sci.* 22 (1999) 221–226.